Thermodynamics of Charged Nanoparticle Adsorption on Charge-Neutral Membranes: A Simulation Study

Yang Li and Ning Gu*

State Key Laboratory of Bioelectronics and Jiangsu Laboratory for Biomaterials and Devices, Southeast University, Nanjing 210096, P. R. China

Received: May 15, 2009; Revised Manuscript Received: December 27, 2009

The interactions between charged nanoparticles (NPs) and charge-neutral phospholipid membranes are investigated by coarse-grained molecular dynamics simulations. Three kinds of nanoparticles are modeled with different surface charge densities: the uncharged one, the positively charged one, and the negatively charged one. We find that the electrostatic attraction improves the adhesion of a charged nanoparticle to the membrane. With the increase of electrostatic energy, a charged NP can be almost fully wrapped by the membrane. In addition, analyses of structural variations suggest that the adhesion of a charged NP induces a local transition in fluid bilayers. Some thermodynamic quantities such as free energy, entropy, and enthalpy are also obtained to explain the process of NPs binding. Furthermore, the bending energy of wrapping of NPs against the electrostatic potential energy is also discussed based on the Helfrich theory, indicating that the driving force of the wrap originates from the gain in electrostatic energy at the cost of the elastic energy of biomembranes. Our observations shed light on the origin of experiments of the wrap as well as the mechanism of structural transitions of membranes due to the electrostatic binding.

Introduction

Electrostatic adsorption of biomolecules or nanoparticles onto lipid membranes is of great biological and technological importance. Understanding the role of electrostatic interactions in bioadhesion may help to elucidate the physiochemical basis of the cell signaling pathway on therapeutic devices.[1] Different from ions, the interaction of nanoparticles with flexible interfaces is expected to be more complex. A great deal of experimental evidence has suggested that the adsorption of a charged nanoparticle disturbs flexible biomembranes.[2−4] Some biological processes, such as the endocytosis of lipid−DNA complexes[5] and the internalization of some viruses,[6] appear to proceed via electrostatic interactions.

There have been quite a number of experimental studies on the interaction of charged NPs with oppositely charged lipid membranes in the last years.[3] Yet, studies involving the interaction of charge-neutral lipid bilayers with charged nanoparticles are still rare. Recent studies have reported that the adsorption of charged NPs onto lipids can induce a surface reconstruction of phospholipid membranes.[7,8] The local patchiness of lipid bilayers mainly depends on the charge of NPs, indicating that the adsorption of charged NPs can probably lead to some unusual effects on the charge-neutral lipids. Furthermore, the uptake mechanism of charged NPs by phospholipid membranes also awaits consensus.

The high complexity of the real biological situation renders a clear extraction of underlying physical principles difficult, and it is not obvious whether an explanation in terms of such principles is sufficient via experimental approaches. As a supplementary means of experiments, theoretical and computational simulation techniques such as the Poisson−Boltzmann (PB) theory,[9] molecular dynamics simulations,[10,11] and other statistical mechanical approaches[12,13] provide some intuitionistic information for these microscale studies. A number of theoretical studies on the interaction of colloids or nanosized particles with flexible membranes have been considered, involving the bending of the membrane in the presence of nanoparticles,[12,14−17] which is regulated by the particle size,[13,18] charge density,[19−22] and flexibility of the membrane.[10] Although those theoretical approaches have been extensively used to study the interactions between charged NPs and oppositely charged lipid membranes, there are few simulations to address the mechanism of interactions between charged NPs and charge-neutral lipid bilayers.

Motivated by the above problems, the specific objective in this paper is to investigate the role of the electrostatic interaction between charged nanoparticles and charge-neutral lipid bilayers in the adsorption and wrap process. Different types of nanoparticles are modeled, and several coarse-grained molecular dynamics simulations are performed. As a result, structure variations of lipid bilayers as well as some thermodynamics parameters have been obtained to shed light on the mechanism of the wrap. Our results represent a more detailed view of the charged NP−bilayer interaction.

Methods

Atomistic simulations reveal maximum details but are restricted to small length and time scales. In view of the relatively large length and time scales of the biological phenomenon in our simulations, a coarse-grained (CG) lipid model (dipalmitoylphosphatidylcholine or DPPC) was employed for its ability to reproduce experimental properties of various lipid assemblies.[23] Force field parameters and further information on the CG model are available in the Supporting Information, SI_1. A solid, nearly spherical nanoparticle was modeled as a face-center-cubic lattice. One nanoparticle with the diameter of ∼6.8 nm consists of 2971 beads, which are constrained to move as a rigid body. There are three types of nanoparticles in our simulations: the uncharged one, the positively charged one, and the negatively charged one. An uncharged nanoparticle, which

* Corresponding author. E-mail: guning@seu.edu.cn.

10.1021/jp904550b
Published on Web 02/10/2010

TABLE 1: Nanoparticles Properties and Simulation Conditions

NP type[a]	e_b (e)	ρ_e (e/nm^2)	T^b (ns)	F^c (kJ/mol nm^2)	N^d
UN	0	0	100	7500	120
P	+0.5	+3.0	120	11500	120
	+1.0	+6.0	120	13500	120
	+1.5	+9.1	160	15500	120
	+2.0	+12.1	220	17500	120
N	−0.5	−3.0	120	11500	120
	−1.0	−6.0	160	13500	120
	−1.5	−9.1	200	15500	120
	−2.0	−12.1	320	17500	120

[a] NP type: "UN" means uncharged NPs; "P" means positively charged NPs; "N" means negatively charged NPs. [b] The full run time of simulations. [c] Force constants of umbrella sampling simulations. [d] Total number of sampling windows.

was modeled as a hydrophilic one, consists of Marrink's nonpolar (Nda) beads. A charged nanoparticle consists of two kinds of beads, charged (Qda) beads for the surface part and nonpolar (Nda) beads for the inner part. The discrete surface charges were modeled in terms of the nature of biomolecules and those NPs of surface functionalization. The number density of surface charges can be calculated by $\rho_e = Ne_b/S_{np}$, where N is the number of surface beads, e_b is the reduced charge of one surface bead, and S_{np} is the surface area of NPs. The different surface charge densities of NPs considered in this paper are shown in Table 1. Here, it should be pointed out that the highest value of charge densities is only an ideal case in the simulations but experimentally unreasonable due to the limited steric space of functionalized groups.[4]

A cubic periodic box with cell dimensions of 38.1 × 37.5 × 29.3 nm^3 was constructed at the origin, including ~290 000 CG water beads and a patch of biomembrane of 4608 CG lipids. The equilibrated nanoparticle was positioned at a distance of ~8.5 nm above the center of bilayer. For charged nanoparticle cases, enough counterions were added to neutralize the system. To facilitate the following discussion, we define the midplane of the lipid bilayer as the $x-y$ plane and introduce the z-axis which is perpendicular to the bilayer surface. The equilibration run times are shown in Table 1 for different simulations.

For all simulations, a Berendsen thermostat/barostat[24] was used to maintain a constant temperature (T) of 323 K and a constant pressure (p) of 1 atm in the NpT ensemble. A cutoff of 1.2 nm was used for van der Waals (vdW) interactions, and the Lennard−Jones potential was smoothly shifted to zero between 0.9 and 1.2 nm to reduce the cutoff noise. For electrostatic interactions, the Coulombic potential, with a cutoff of 1.2 nm, was also smoothly shifted to zero from 0 to 1.2 nm. All the simulations had been performed with the GROMACS simulation package.[25]

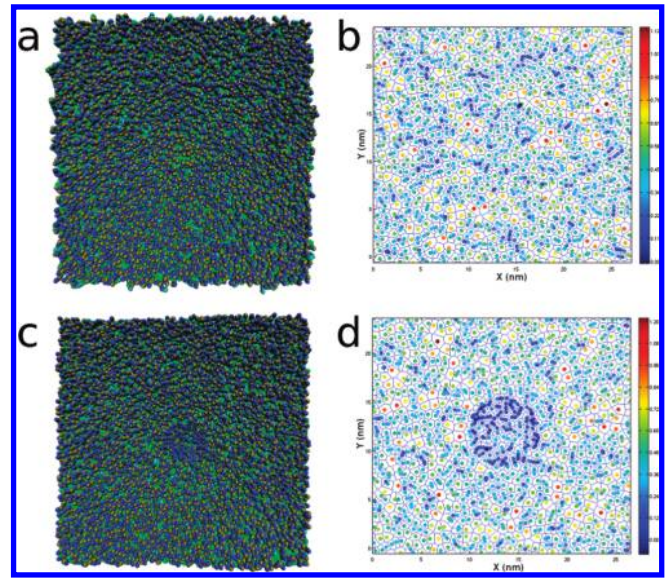

Figure 2. Visualization of the area per lipid of the DPPC bilayer, in which (a),(b) for a cationic NP case of $\rho_e = +3.0$ e/nm^2 and (c), (d) for an anionic NP case of $\rho_e = -3.0$ e/nm^2. Panels (a) and (c) show the configuration of a lipid bilayer. Panels (b) and (d) show the area per lipid in one monolayer, determined using a Voronoi tessellation of the c.o.m. coordinates of the headgroup.

Results and Discussion

In this section, a comparison of the interactions between the membrane and different NPs is given, and structural variations of the membrane characterized by area per lipid and average order parameter are analyzed. Different binding configurations of a NP on a lipid membrane are shown in Figure 1. Because of its hydrophilicity, an uncharged nanoparticle prefers to remain in water over adsorbing onto the lipid bilayer (Figure 1(a)). Instead, charged nanoparticles, driven by the electrostatic interactions, can adsorb on the membrane. The adsorption of charged NPs induces the membrane deformation. It is clear that the membrane deformation depends significantly on the surface charge densities of NPs. In the following, we examine the response of the membrane to an adhered nanoparticle. Two charged NP cases of $\rho_e = \pm 3.0$ e/nm^2 are discussed, respectively.

The adsorption of charged NPs disturbs the lipid bilayer and has an influence upon the density distribution of head groups of lipids. The variations of lipids induced by the adsorption of NPs around the adhering position are shown in Figure 2(a) and (c). Here, the distribution of head groups is calculated using a 2D Voronoi tessellation of the center-of-mass (c.o.m.) positions of lipids.[26] The Voronoi diagrams show that there is a significant difference between cationic NPs and anionic NPs. The density of head groups of lipids around the adhering position is merely affected by the adsorption of a positively charged NP (Figure

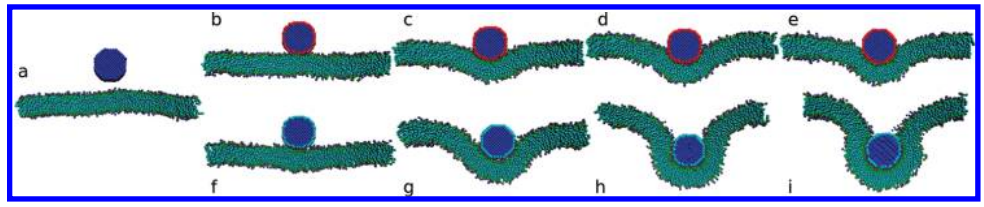

Figure 1. Trajectory snapshots of simulations of three types of NPs. Panel (a) shows the snapshot of the uncharged NP case. Panels (b)−(e) for positively charged NP cases in which ρ_e includes: +3.0 e/nm^2, +6.0 e/nm^2, +9.1 e/nm^2, and +12.1 e/nm^2. Panels (f)−(i) for negatively charged NP cases in which ρ_e includes −3.0 e/nm^2, −6.0 e/nm^2, −9.1 e/nm^2, and −12.1 e/nm^2. A blue bead cluster represents a hydrophilic nanoparticle; red beads represent a positively charged surface; cyan beads represent a negatively charged surface; green beads represent a DPPC bilayer. The explicit water and ions are omitted for clarity. The images are created with VMD.[37]

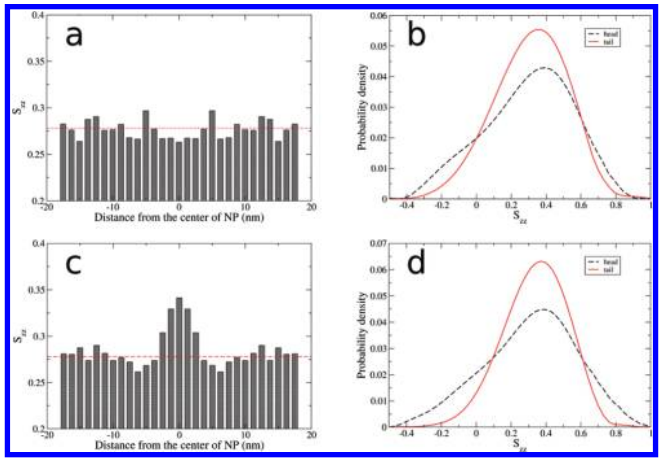

Figure 3. Order parameters of the membrane, in which (a),(b) for a cationic NP case of $\rho_e = +3.0$ e/nm^2 and (c),(d) for an anionic NP case of $\rho_e = -3.0$ e/nm^2. Panels (a) and (c) show the distributions of order parameter S_{zz} of the membrane. Panels (b) and (d) show the probability distributions of the average order parameters for the trajectory, smoothed by a Gaussian fitting.

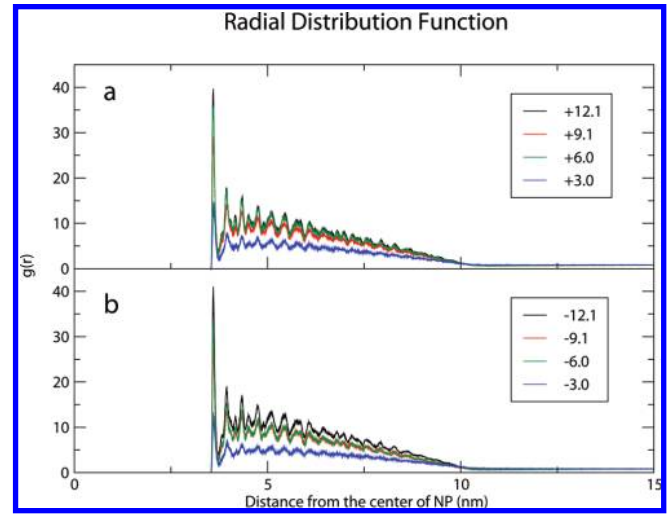

Figure 4. RDFs for (a) NPs of positive charge with counterions and (b) NPs of negative charge with counterions, averaged over the last 40 ns. The surface charge densities ρ_e of involved NPs include: $\pm$12.1 e/nm^2, $\pm$9.1 e/nm^2, $\pm$6.0 e/nm^2, and $\pm$3.0 e/nm^2.

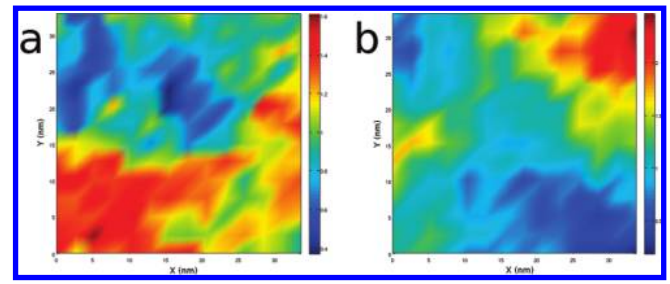

Figure 5. Undulations of membranes. (a) for a cationic NP case of $\rho_e = +3.0$ e/nm^2 and (b) for a anionic NP case of $\rho_e = -3.0$ e/nm^2.

2(b)). Yet, the adhesion of a negatively charged NP induces the formation of a high density domain of head groups around the nanoparticle (Figure 2(d)), where the area of head groups decreases.

Large differences in packing imply that different order transitions of lipids may occur in those regions. The average order parameter for lipid molecules has been calculated as a measure of lipids' packing. It is given by $S_{zz} = 1/2\langle 3\cos^2\theta_i - 1\rangle_i$, where θ_i is the tilt angle between the bilayer normal (lying along the z direction) and the molecular axis which connects the neighboring atoms $i-1$ and $i+1$, and $\langle\cdot\rangle_i$ denotes an average over all of the atoms in the lipid. The extremum values of S_{zz} are 1 and -0.5, corresponding to a perfectly ordered state and a conformation perpendicular to the membrane normal, respectively, and lack of order is characterized by $S_{zz} = 0$.[26] For frames in the simulation trajectory, we split up the membrane into some concentric ring slices around the NP, and the local transition of the bilayer can also be obtained by calculating the distribution of order parameters of lipids.

Due to the electrostatic interaction, the binding of a charged nanoparticle alters the tilt angle of the phosphocholine (PC) headgroup of DPPC lipids, which is terminated by an electric dipole of positively charged choline and negatively charged phosphate, N^+-P^-. Correspondingly, the local disordered variations of lipids in the adsorption region of positively charged NPs can be seen in Figure 3(a), and the local high ordered variations of lipids in the adsorption region of negatively charged NPs is shown in Figure 3(c). In addition to the universal presence of van der Waals forces, the driving force comes from the electrostatic attraction between the charged surface components of NPs and the charged components of head groups of lipids.[27] The attraction between the positively charged surface of NPs and the P^- terminus of lipids can increase the tilt angle (Figure 3(a)), and the attraction between the negatively charged surface of NPs and the N^+ terminus of lipids reduces the tilt angle of the dipole above the average angle (Figure 3(c)). As a result, these changes could switch the phase state of a phospholipid bilayer.[7,8,28]

Further, the structure of the membrane would be affected by changes of the tilt angle of lipids. For the case of cationic NPs, the increased tilt angle of the headgroup makes lipids reversal-conically shaped, which could increase the area of the head groups. Conversely, for the case of anionic NPs, the reduced tilt angle of the headgroup makes the lipid molecules conically shaped, which decreases the area of the headgroup. Moreover, these changed lipids, due to the adsorption of anionic NPs, are more prone to forming a curved membrane than those affected by cationic NPs. Therefore, head groups of lipids around the anionic NP preferably concentrate to form a domain. The change in the upper leaflet induces the asymmetric lipid distributions of biomembranes and promotes the bilayer bending to wrap the anionic NPs.[29] It could be one reason that the adsorption of anionic NPs has a stronger influence on the structural changes of membranes than cationic NPs (Supporting Information, SI_2).

The structural variation in order parameters of the lipid bilayers is a local phenomenon, which is demonstrated by the profiles of the probability distributions of the average order parameters for the trajectory (Figure 3(b) and (d)). There exists merely a slight difference in the part of the head groups between the case of cationic NPs and anionic NPs. Here, two factors might help us explain this: (i) For charged NPs, some oppositely charged counterions, which are loosely bound to the surface of NPs, screen the range of electrostatic interactions. The radial distribution functions (RDFs) of counterions around NPs are shown in Figure 4. (ii) Since a membrane is in its fluid state, the lipids are, in principle, responsive as a charged object approaches. In the simulation, the adsorption of charged NPs can suppress local lipid undulations but stimulate those lipids around the NP to protrude out of the bilayer (Figure 5). The fluctuation in the system becomes strong, obscuring any possible difference in the probability distributions of the different domains.[9,14] This suppressing effect in the adhering region is

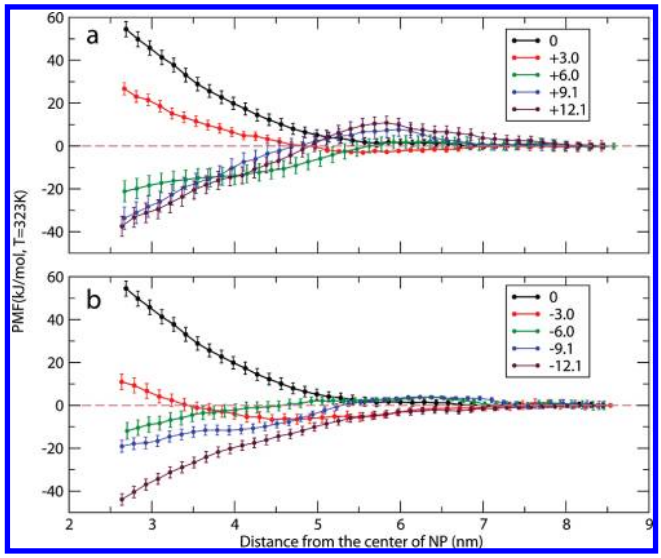

Figure 6. PMF of a NP as a function of its distance from the midplane of the DPPC bilayer. Panel (a) shows PMF of a NP of positive charge. Panel (b) shows PMF of a NP of negative charge. The ρ_e of involved NPs includes: ± 3.0 e/nm^2, ± 6.0 e/nm^2, ± 9.1 e/nm^2, and ± 12.1 e/nm^2. Vertical bars represent standard errors.

more visible in the case of anionic NPs (Figure 5(b)) than that of cationic NPs (Figure 5(a)). For cationic NPs at the low surface charge density, the weak attraction of the NP bilayer cannot make a strong binding on the membrane like that of anionic NPs (details in Sec. PMF). Such a weak binding of cationic NPs on lipids promotes the local undulation of lipids in the adhering region rather than suppressing them.

PMF. Here, we focus on the thermodynamic function which characterizes systems in equilibrium. To gain a better understanding of the relationship between the surface charge characteristics of NPs and responses of biomembranes to the interactions, we extract free energy profiles of adsorptions in the form of potentials of mean force (PMF)[30] as a means of comparing energetic costs of different nanoparticles. The reaction coordinate was defined as the axis connecting the c.o.m. of NP with the c.o.m. of bilayers. Umbrella sampling (US)[31] simulations were applied, respectively, to obtain biased position histograms along the reaction coordinate. During the US simulations, a series of force constants for different kinds of nanoparticles were used with a spacing of 0.02 nm between biasing harmonic potentials, shown in Table 1. Each umbrella sampling simulation was preformed separately for 2 ns. For the analysis, the weighted histogram analysis method (WHAM) was applied to calculate the PMF profiles,[32] and statistical errors of PMF profiles were computed using bootstrap analysis.[33] The PMF of nanoparticles adsorbing on the membrane are displayed in Figure 6, where all PMF are aligned so that they have a value of zero in the water phase ($z \sim 8.5$ nm), and thus all free energy changes are relative to NPs in water.

The equilibrium of the interaction is determined by minimizing its energy. Independent of the surface charge, the interaction between a hydrophilic NP and the membrane is purely repulsive. In the case of the uncharged NP, the onset of the repulsion appears at $z \sim 5.7$ nm, which is in agreement with the dispersion of the headgroup locations for an unperturbed membrane.[20]

The electrostatic attraction improves the adhesion of a charged NP to the membrane. However, PMF of charged NPs indicate that there is an energy barrier existing to suppress a binding of NPs. For the case of cationic NPs, the energy barrier results from the repulsion between positively charged surface and positively charged choline groups (N^+) of lipids and also from the bending energy of membranes. The larger the surface charge density of NPs, the higher repulsive energy barrier there is (Figure 6). In spite of this, the repulsive energy barrier can still be overcome by the electrostatic attraction. Consequently, a NP of positive charge can also be partially wrapped. Similarly, the energy barrier also exists in the system of anionic NPs. Besides from the bending energy of membranes, the energy barrier comes from the repulsion between the negatively charged surface of NPs and negatively charged phosphate groups (P^-) of lipids. Compared with the case of cationic nanoparticles, the repulsive energy barrier in the anionic nanoparticle's case is small. This free energy difference between cationic NPs and anionic NPs is due to the components alignment of lipids, which induces the different interaction of charged NPs with the electric dipole of the headgroup of a lipid (Supporting Information, SI_2(c)). As a result, the adsorption of positively charged NPs suppresses the wrap of the membrane, whereas the negatively charged NPs' adhesion promotes the wrap.

When the surface charge density is low ($\rho_e = \pm 3.0$ e/nm^2), the adsorption of charged NPs only induces the membrane bending instead of a significant wrap (Figure 1(b) and (f)), which means that the bending energy barrier of the membrane is still too large to be overcome by electrostatic attractions. However, the electrostatic contribution favors highly curved structures of the lipid bilayer, allowing the formation of a bud wrapping the NP from a flat membrane at the situations of high surface charge densities. These transitions can be seen in Figure 1(c)−(e) and (g)−(i). Take an example of PMF of $\rho_e = \pm 6.0$ e/nm^2: the decreasing tendency of the PMF profile starts at the $z \sim 5.5$ nm, indicating the driving force of interactions is no longer the bending energy but the electrostatic attraction. Similar are PMF of $\rho_e = \pm 9.1$ e/nm^2 and $\rho_e = \pm 12.1$ e/nm^2. With the increase of the adhesion energy, a charged NP goes deeper into the region and can be almost fully wrapped at a higher density of surface charge.

Entropy and Enthalpy. We then extract the entropic and enthalpic components of the free energy to quantify their contributions to the interactions. One can use numerical approximations to obtain these thermodynamic quantities through their temperature dependence of free energy[34]

$$-T\Delta S = T\frac{dG}{dT} \approx \frac{T}{2\Delta T}(G(T+\Delta T) - G(T-\Delta T))$$
$$\Delta H = \Delta G + T\Delta S \quad (1)$$

Several umbrella sampling calculations are carried out, respectively, at three different temperatures (319, 323, and 327 K), and the entropic and enthalpic contributions to the free energy are evaluated using eq 1. Similar to PMFs, these profiles in Figure 7 are also aligned to zero. Entropy and enthalpy estimates reflect the origin of energy barriers but also suffer from statistical inaccuracy.

Here we still consider two NPs of $\rho_e = \pm 3.0$ e/nm^2, respectively. Shown in Figure 7, the adsorption of charged NPs on biomembranes is a delicate interplay between entropic and energetic components. For the adsorption of NPs of positive charge (Figure 7(a)), the free energy of a NP transferring from water bulk to the surface of the membrane is favorable, but the enthalpy component is not because of the repulsive interaction between the positively charged surface of NPs and the positively charged choline group of lipids. Nevertheless, the binding is encouraged by an entropy

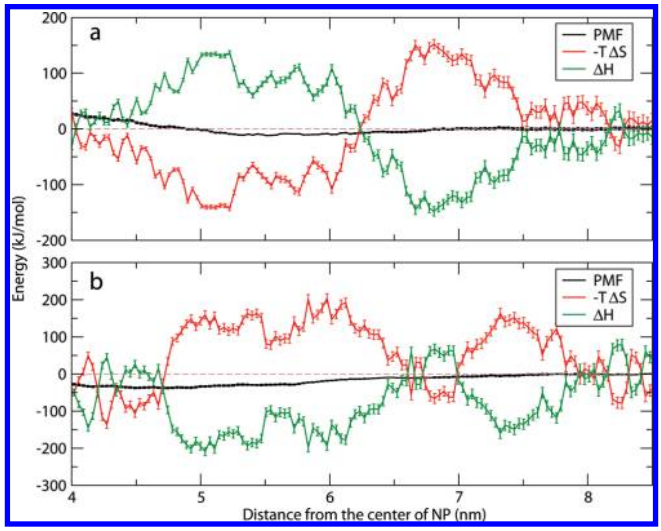

Figure 7. Entropy and enthalpy components of the adsorption of a NP from water onto the membrane. Panel (a) shows the decomposition of the PMF of a positively charged NP of $\rho_e = +3.0$ e/nm^2. Panel (b) shows the decomposition of the PMF of a negatively charged NP of $\rho_e = -3.0$ e/nm^2. Vertical bars represent standard errors.

change; as it were, this process should be endothermic. On the contrary, the adhesion of negatively charged NPs undergoes a quite different process, shown in Figure 7(b). The decomposition profiles of free energy reveal a significant contribution from entropy. The entropic cost may result partly from high ordered changes of lipids in the adhering region and partly from release of water from the headgroup of lipids when nanoparticles bind.[8] The binding of negatively charged NPs is dominated by the favorable enthalpy change, indicating that this process should be exothermic. This is in a qualitative agreement with the recent results from the work of Wang and collaborators.[8]

Besides, we speculate that both of the profiles go through a process of entropy gain when a charged NP moves from the water bulk to the surface of the membrane. Far from the membrane, the distribution of counterions around a particle is spherically symmetric. When a particle is close to the membrane, the distribution of counterions around becomes perturbed. Some bound counterions on the NP can unbind to the water, giving rise to the contribution of entropy.[9] However, the cooperativity of this process has been complicated by the participation of lipids; no quantitative explanation is presented at this time.

System Energy. The competition between the electrostatic and elastic contributions to the free energy dominates the range of lipid rearrangements which results in the NP's encapsulation. These equilibrium configurations can be determined by minimizing the macroscopic free energy. This approach has been used for determining the equilibrium conformations of the wrap of a particle by biomembranes.[13,16] To further explore the influences of charged NPs upon the biomembranes, we now investigate the wrap of membranes in a macroscopic view.

Since the tensionless membrane has been used in all simulations, the process of interplays of NPs and membranes can be understood as a balance of the following two energy contributions: (i) binding driven by the attractive energy and (ii) an opposed effect due to the bending energy of membranes.[13] The bending energy per unit area can be described using the standard Helfrich expression[35]

$$f_{bend} = \frac{1}{2}k_c(2H + c_0)^2 + \bar{k}K \qquad (2)$$

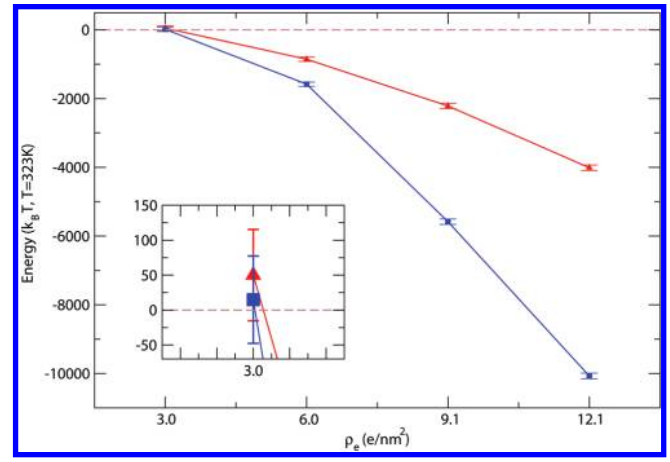

Figure 8. System energy as a function of the surface charge density of NPs. Red triangles represent cationic NP cases, and blue cubes represent anionic NP cases. The inset shows the cases of $\rho_e = \pm 3.0$ e/nm^2. Vertical bars represent standard errors.

where k_c and $\bar{k}$ are bending rigidities; c_0 is the spontaneous curvature of the membrane; and H and K are the mean and Gaussian curvature of the membrane surface, respectively. Since the surface integral of Gaussian curvature is constant with respect to deformations of the membrane based on the Gauss−Bonet theorem, there is only the contribution of the mean curvature to the wrap of the membrane.[16] On the other hand, the binding energy of the membrane depends on the van der Waals potential and electrostatic potential. Considering the repulsive nature of charged neutral nanoparticles working on biomembranes, the binding energy of charged NPs on a lipid bilayer can be represented as

$$F_{adh} = F_{lipid}^{coul} + F_{lipid}^{vdw} - F_{sol}^{vdw} \qquad (3)$$

where F_{lipid}^{coul} is the electrostatic energy between the NP and the membrane; F_{lipid}^{vdw} is the vdW potential energy between NP and lipids; and F_{sol}^{vdw} is the vdW potential energy between the NP and solvent. Then the total energy of a membrane is

$$F = -\int f_{bend} dA + F_{adh} \qquad (4)$$

where A is the contact area.

The total energy of membranes as a function of surface charge densities has been shown in Figure 8. The NP-wrapped state is electrostatically favorable but entails a penalty in bending energy of the membrane. Particle wrapping should occur when the electrostatic energy gain due to adhesion exceeds the cost of bending. Quite generally then, a transition from the planar to the wrapped geometry takes place when the surface charge density exceeds a certain "crossover" value. Here, we define the "crossover" charge density of NPs, ρ_e^*, and, correspondingly, the necessary adhesion energy per unit area, f_{adh}^*, where $f_{adh}^* = F_{adh}^*/A$. We estimate that the value of ρ_e^* is ~3.0 e/nm^2 and the f_{adh}^* for wrapping is ~$0.43k_BT$/nm^2 (k_B is the Boltzmann constant and T is the system temperature). Comparing with the estimated value, it is worth noting that the real crossover value should be larger for cationic NPs and smaller for anionic NPs (Supporting Information, SI_3). The f_{adh}^* is consistent with the predicted energy value in view of binding energy,[13] but the ρ_e^* is somewhat larger than the predicted charge value by Harries.[21] Since a mixed lipid bilayer is used in the work of Harries

composed of neutral and charged lipids, the attraction of charged NPs and charged lipids cannot be neglected in the interaction, and different from their Poisson−Boltzmann model,[21] the surface charge of NPs in our simulations has a realistic discrete representation, which could modulate the counterions' distribution which can also affect the charged NP's behavior.[9,36]

Furthermore, the strength of the attraction increases with the surface charge density (Figure 8). Under the present conditions, the depth of the attractive system energy increases nonlinearly at low densities of surface charges but almost linearly at high densities of surface charge. In our simulations, even the condition of a highest density of surface charges cannot drive a full wrap transition. Nevertheless, recent theoretical analysis shows that, when the membrane tension is sufficiently low or the particle is small enough, bending of the membrane becomes an important contribution which can be strong enough to suppress wrapping.[13] It is clearly shown that the two principle curvatures form in the neck region of the lipid bilayer (Figure 1(i)). As a result, the bending stiffness prevents any "kink" in the membrane profile at the line of contact, which might prevent the wrap further.[29]

Conclusion

To summarize, we have investigated interactions between charged NPs and electroneutral phospholipid bilayers. There are three types of charged NPs with different surface charge densities we studied: the uncharged one, the positively charged one, and the negatively charged one. The results of interactions show that the electrostatic attraction improves the adhesion of a charged NP to the membrane. Moreover, comparative analysis of the structural variations of membranes reveals that the nonspecific adsorption of charged nanoparticles has significant effects on the physical characteristic of the membrane. The adsorption of cationic nanoparticles induces the local disordered transition in the adhering region of the membrane, whereas nanoparticles of negative charge induce the formation of the high ordered region in fluid bilayers. Further, we find that the adsorption of cationic/anionic nanoparticles on the membrane plays a different role of suppressing or promoting the membrane wrapping. Such results are discussed in terms of free energy, entropy, and enthalpy. There exists an energy barrier between lipids and charged NPs, which comes partly from the bending energy of the membrane and partly from the repulsion of the oppositely charged components of the headgroup of lipids. We witness that the adhesion of positively charged NPs is entropy favorable, which works against the energy cost. By contrast, NPs of negative charge are driven by the enthalpy, which suffers from the entropic penalty. Elastic energy analysis indicates that the driving force for the formation of a wrapped state originates from the gain in electrostatic energy at the expense of the elastic energy of biomembranes. Thus we conclude that surface charge plays a crucial role in the interaction of charged NPs and charge-neutral phospholipid bilayers. These studies are consistent with experimental observations and give insight into the origin of the membrane's wrap of charged NPs.

Acknowledgment. This work is supported by grants from the National Important Basic Research Program of China (Grants 2006CB933206 and 2006CB705606) and NFC60725101. The authors thank Dr. Lanyuan Lu and Wen-de Tian for valuable discussions.

Supporting Information Available: Details of system energy contributions of different components obtained from these interactions. This material is available free of charge via the Internet at http://pubs.acs.org.

References and Notes

(1) Nel, A.; Xia, T.; Madler, L.; Li, N. *Science* **2006**, *311*, 622–627.
(2) Hong, S.; Bielinska, A.; Mecke, A.; Keszler, B.; Beals, J.; Shi, X.; Balogh, L.; Orr, B.; Baker, J.; Holl, M. *Bioconjugate Chem.* **2004**, *15*, 774–782.
(3) Leroueil, P.; Berry, S.; Duthie, K.; Han, G.; Rotello, V.; McNerny, D.; Baker, J.; Orr, B.; BanaszakHoll, M. *Nano Lett.* **2008**, *8*, 420–424.
(4) Goodman, C.; McCusker, C.; Yilmaz, T.; Rotello, V. *Bioconjugate Chem.* **2004**, *15*, 897–900.
(5) Pedroso de Lima, M.; Simões, S.; Pires, P.; Faneca, H.; Düzgüneş, N. *Adv. Drug Delivery Rev.* **2001**, *47*, 277–294.
(6) Garoff, H.; Hewson, R.; Opstelten, D. *Microbiol. Mol. Biol. Rev.* **1998**, *62*, 1171–1190.
(7) Zhang, L.; Granick, S. *Nano Lett.* **2006**, *6*, 694–698.
(8) Wang, B.; Zhang, L.; Bae, S.; Granick, S. *Proc. Natl. Acad. Sci.* **2008**, *105*, 18171.
(9) Messina, R. *J. Phys.: Condens. Matter* **2009**, *21* (18pp), 113102.
(10) Noguchi, H.; Takasu, M. *Biophys. J.* **2002**, *83*, 299–308.
(11) Tian, W.; Ma, Y. *J. Phys. Chem. B* **2009**, *113*, 13161–13170.
(12) Lipowsky, R.; Dobereiner, H. G. *Europhys. Lett.* **1998**, *43*, 219–225.
(13) Deserno, M. *Phys. Rev. E* **2004**, *69*, 031903.
(14) May, S. *Curr. Opin. Colloid Interface Sci.* **2000**, *5*, 244–249.
(15) Livadaru, L.; Kovalenko, A. *Nano Lett.* **2006**, *6*, 78–83.
(16) Smith, K.; Jasnow, D.; Balazs, A. *J. Chem. Phys.* **2007**, *127*, 084703.
(17) Oettel, M.; Dietrich, S. *Langmuir* **2008**, *24*, 1425–1441.
(18) Ginzburg, V.; Balijepalli, S. *Nano Lett.* **2007**, *7*, 3716–3722.
(19) Fleck, C. C.; Netz, R. R. *Europhys. Lett.* **2004**, *67*, 314–320.
(20) Dias, R. S.; Linse, P. *Biophys. J.* **2008**, *94*, 3760–3768.
(21) Harries, D.; Ben-Shaul, A.; Szleifer, I. *J. Phys. Chem. B* **2004**, *108*, 1491–1496.
(22) Lee, H.; Larson, R. G. *J. Phys. Chem. B* **2006**, *110*, 18204–18211.
(23) Marrink, S. J.; de Vries, A. H.; Mark, A. E. *J. Phys. Chem. B* **2004**, *108*, 750–760.
(24) Berendsen, H. J. C.; Postma, J. P. M.; van Gunsteren, W. F.; DiNola, A.; Haak, J. R. *J. Chem. Phys.* **1984**, *81*, 3684–3690.
(25) Lindahl, E.; Hess, B.; van der Spoel, D. *J. Mol. Model.* **2001**, *7*, 306–317.
(26) Murtola, T.; Róg, T.; Falck, E.; Karttunen, M.; Vattulainen, I. *Phys. Rev. Lett.* **2006**, *97*, 238102.
(27) Cha, T.; Guo, A.; Zhu, X. *Biophys. J.* **2006**, *90*, 1270–1274.
(28) Somerharju, P.; Virtanen, J.; Cheng, K. *Biochem. Biophys. Acta, Mol. Cell Biol. Lipids* **1999**, *1440*, 32–48.
(29) Cooke, I. R.; Deserno, M. *Biophys. J.* **2006**, *91*, 487–495.
(30) Roux, B. *Comput. Phys. Commun.* **1995**, *91*, 275–282.
(31) Torrie, G. M.; Valleau, J. P. *Chem. Phys. Lett.* **1974**, *28*, 578–581.
(32) Kumar, S.; Rosenberg, J.; Bouzida, D.; Swendsen, R.; Kollman, P. *J. Comput. Chem.* **1992**, *13*, 1011–1021.
(33) Allen, M.; Tildesley, D. *Computer simulation of liquids*; Oxford University Press: USA, 1990.
(34) MacCallum, J. L.; Tieleman, D. P. *J. Am. Chem. Soc.* **2006**, *128*, 125–130.
(35) Helfrich, W. *Z. Naturforsch. Teil C: Biochem., Biophys., Biol., Virol.* **1973**, *28*, 693.
(36) Grosberg, A.; Nguyen, T.; Shklovskii, B. *Rev. Mod. Phys.* **2002**, *74*, 329–345.
(37) Humphrey, W.; Dalke, A.; Schulten, K. *J. Mol. Graphics* **1996**, *14*, 33–38.

JP904550B